DEVELOPMENT AND VERIFICATION OF DESIGN METHODS FOR DUCTS IN A SPACE NUCLEAR SHIELD

R. J. Cerbone, W. E. Selph, and P. A. Read

Gulf Radiation Technology
A Division of Gulf Energy & Environmental Systems Incorporated

A practical method for computing the effectiveness of a space nuclear shield perforated by small tubing and cavities has been developed and tested.

Analysis of ducts and voids in a shield cannot be performed using the two-dimensional transport methods that are presently the most efficient means of analyzing reactor and shield problems. A three-dimensional Monte Carlo analysis is the only rigorous approach; however, it is too costly to consider in tradeoff studies. Methods are needed that will provide reasonable accuracy at a moderate cost.

Our approach to the problem is to use solutions of a two-dimensional transport code and evaluate perturbations of that solution using last flight estimates and other kernel integration techniques. In general, perturbations are viewed as a change in the source strength of scattered radiation and a change in attenuation properties of the region, and the effect of these changes is evaluated by performing last flight estimates and point kernel integrations. This method has been implemented in a new computer program called DUCT.

Calculations performed with the DUCT code have been compared to experiments conducted at the Gulf Radiation Technology Linac facility. The shield studies involved measurements on a lithium hydride assembly with a sodium filled duct and a NERVA-BATH shield mockup. Comparison has also been made with the MORSE Monte Carlo code. Overall agreement between measurements, DUCT, and MORSE has been better than 10 percent.

1. INTRODUCTION

A variety of techniques are available for estimating radiation streaming down ducts. Some of these techniques are summarized in ref. 1. The majority of the duct streaming work, both experimental and analytical, has been concentrated on void ducts whose dimensions are large compared to the radiation mean free path in the material. For these cases, the radiation incident on the mouth of the duct is the predominant source of radiation reaching the duct exit either by direct streaming or by albedo from the duct wall. Relatively simplified analyses of these two components provide answers that are in reasonable agreement with experiment for cases such as shelter entry ways or beam ports through reactor shields.

Ducts through shields in space reactors are, however, more likely to be filled either by metal or by some fluid so that radiative exchange between the duct material and the shield material becomes an important contribution to the radiation exiting from the duct. Evaluating the effect of a filled duct is therefore a more complicated process and is not amenable to an unsophisticated approach. An exact solution requires the use of a radiation transport code with a three-dimensional generalized geometry capability (a Monte Carlo code). The motive behind the work described here is to arrive at an approximate method that can be applied to iterative design studies without the large expenditure of computer time required for a series of Monte Carlo calculations.

This research was divided into four parts; namely,

1. Formulation and programming of a code for calculating the effects of shield irregularities on the space craft environment. This method consists of using the solution of a two-dimensional transport code as a starting point and making perturbations to that solution to account for shield irregularities such as coolant ducts and other shield perturbations.
2. Performance of analytical tests to determine the range of validity of the code developed in Part 1.
3. Performance of an experimental program using a geometry and material similar to real space-power shielding problems but "clean" enough to provide a good check on the analysis.
4. Extension of the experimental-analytical comparison to include neutron and secondary gamma production and transport in a NERVA-BATH shield assembly.

2. DEVELOPMENT OF THE DUCT CODE

Except for isolated irregularities, we assume that the shield can be approximated by

use of a two-dimensional model. Neglecting these irregularities, a two-dimensional calculation can be performed using a transport code such as TWOTRAN (ref. 2) or DOT (ref. 3). These codes can be made to generate a "flux tape" which is a complete listing of fluxes within a spatial energy and angle mesh specified in the calculation. The DUCT code that we have written takes these fluxes as input and solves for perturbations in the flux at specified detector points caused by the presence of irregularities in the shield. In the present form, the code only considers cylindrical ducts. In some parts of the code the 2D angular flux mesh is used in a discrete manner, in other parts, interpolations in angle are made. Spatial interpolations are made in all cases and the fixed energy grouping is used throughout.

The primary assumption attendant to the derivation of the method is that the inward-directed current passing through the surface of a duct is obtained by integrating over the angular flux predicted from the unducted 2D solution. In other words, it is assumed that changing the material in the duct region does not change the level of radiation passing into the region. Auxilliary one-dimensional transport calculations in cylindrical geometry show this to be a good approximation.

2.1 ESTIMATOR FOR THE SCATTERED RADIATION

The last collision kernel volume integral is given as

$$\varphi(E)_S = \iiint_{vE'\Omega'} \frac{\varphi(\Omega', r, Z, E')P(E'\Omega' \rightarrow E\Omega)\exp(-b(E'))}{R^2}$$

where

$\varphi(\Omega', r, Z, E')$ are flux components in phase space coordinates in cylindrical geometry centered in dv.

Ω' is direction of incoming flux, and E' is energy of incoming flux.

R is the distance from dv to the detector.

Ω is the direction from dv to the detector.

E is the energy after collision.

$P(E'\Omega' \rightarrow E\Omega)$ is the scattering cross section per steradian per cc for transitions from Ω' to Ω and E' to E. These two transitions are not independent since for a given scattering species the energy lost in a collision depends on the scattering angle. Where dv is filled with a variety of scattering species more than one E can result from a given incident E' and Ω' flux component.

$b(E')$ is $\Sigma_T(E')R$.

To simplify the evaluation of the last collision integral, group-averaged cross sections and group fluxes are used for both the incident and scattered radiation. This allows us to use the same cross-section set in the perturbation calculation as that used in the 2D transport analysis of the idealized shield.

Another simplification is to restrict the the duct shape to cylinders and divide the duct volume by planes perpendicular to the duct axis. Each of the volume elements can then be treated as an equivalent disk source. The uncollided flux from an isotropic disk source of strength S_A per unit area at a detector on the axis is given by

$$\varphi = \frac{S_A}{2}\left[E_1(\mu t) - E_1(\mu t \sec\theta)\right] ,$$

where μt is the integral of total cross sections along the axis between the two points and θ is the angle between a ray on the axis and a ray from the detector to the outer rim of the disk and the function $E_1(x)$ is given by

$$\int_x^\infty \frac{e^{-t}}{t}\,dt.$$

Using the group averaging approach the flux at a detector on the duct centerline at the exit plane is then given by

$$\varphi_S(g') = \sum_g\sum_m\sum_n P_S(g \rightarrow g', m)\, W_m \varphi_m(n, g)$$
$$*2\pi\Delta t_n\left[E_1(-\mu(g)R(n)) - E_1(-\mu(g)R(n)\sec\theta_n)\right] ,$$

where $P_S(g \rightarrow g', m)$ is the unit volume probability of scattering from group go to group g' from the mth angle to the direction of the detector. $P_S(g \rightarrow g'm)$ is given by

$$P_S(g \rightarrow g'; \theta_S) = \frac{1}{4\pi}\sum_{\ell=0}^{n} S_\ell(g \rightarrow g')P_\ell(\theta_S) ,$$

where

$S_\ell(g \rightarrow g')$ are given by the group average cross sections generated by GGC4.

W_m is the quadrature weight of the mth angle increment = solid angle/4π.

$\varphi_m(n, g)$ is the angular flux at the nth duct point in the mth angle in group g (4π x neutrons cm^{-2} $STER^{-1}$).

$\mu(g)R(n)$ is the total number of mean free paths from the nth duct point to the detector for group g.

2.2 ESTIMATOR FOR THE UNCOLLIDED FLUX TO ON-AXIS DETECTOR

The uncollided flux from radiation passing through the duct wall is given by

$$\varphi(E)_D = \frac{\int\varphi(\Omega, r, Z, E)\bar{\Omega}\cdot\bar{n}\,dS\exp(-\Sigma_r(E)R)}{R^2} ,$$

where

$\varphi(\Omega, r, Z, E)$ are the flux components.

Ω is the direction from the surface element dS to the detector.

n is a unit vector normal to the surface increment.

r, Z are the space coordinates centered in dS. R is the distance from r, Z to the detector.

Using the same numerical approach to evaluate this integral as was used in the scattering calculations detailed above,

$$\varphi_D(g) = \sum_n \frac{\overline{\varphi}(n, g)\Delta S \cos\theta \exp(-\mu(g)R(n))}{R^2(n)}$$

where

ΔS is the duct surface area associated with the particular duct segment.

$\overline{\varphi}(n, g)/4\pi$ is the flux per steradian in the detector direction averaged over ΔS.

θ is the angle between the surface normal and a ray to the detector.

The perturbation caused by the material filling the duct is assumed to express itself as a change in the scattering intensity within that geometric region and as a change in the component which streams from the duct wall to the detector without suffering a collision. The scattered flux is thus obtained by integrating a last flight estimator over the volume based on a collision density given by the unperturbed flux times the differential angular scattering probability. The direct flux is obtained by integrating an uncollided kernel over the surface of the duct where the local source is given by interpolating the 2D fluxes. The perturbation is then obtained by comparing the results of these calculations with calculations where the volume of concern is filled with shield material.

2.3 ESTIMATOR FOR THE UNCOLLIDED COMPONENT FOR OFF-AXIS DETECTORS

Formulations have been made for calculating the uncollided component to detectors off the duct axis. It will be recalled that the basic method is capable of calculating both a collided and uncollided component on the duct axis, but for off-axis detectors it can only calculate the collided contribution. The formulation presented here permits an estimate to be made of the enhanced penetration of flux vectors whose paths lie partially within the duct and partially within the surrounding shield.

The complicated geometry is one of the major obstacles in formulating the estimator. The effective area on the duct wall that can radiate toward the detector is given by integrating over all the surface areas associated with the duct increment whose normal has a component in the detector direction

$$\int_{\Delta A} \bar{r} \cdot \bar{n}\, dA \ ,$$

where $\bar{r}$ is a unit vector in the direction of the detector and $\bar{n}$ is a unit vector normal to the tangent plane to the surface. It is assumed that the direction $\bar{r}$ is essentially the same for all points on the duct increment or that the distance to the detector is large when compared to the radius of the duct.

It is possible to evaluate the integral over the appropriate area and multiply by the flux vector to get a total "source" in the detector direction but this is inappropriate because it does not account for the varying path lengths through the duct. To account properly for the varying path lengths the surface must be split into azimuthal increments. Some trial and error cases showed that splitting the 180° band into six equal 30° increments provides a reasonable approximation of the projected area. The actual area of each increment is $\frac{\pi r}{6}\Delta t$ and the flux contribution to the detector is

$$\varphi(E)_o = \varphi(\bar{r}, E)\bar{r} \cdot \bar{n} \frac{\pi r}{6} e^{-b_1/R^2}$$

where Δt is the length increment, R is the detector-to-area increment separation distance, and b_1 is the integral of total cross section along R.

3. CALCULATIONS OF THE LITHIUM HYDRIDE SHIELD EXPERIMENT

The first test for the DUCT code was an attempt to simulate a neutron shield applicable to to the SNAP type shield. This shield consists of a lithium hydride shield with sodium coolant holes.

The shield was represented in the DOT calculation as a cylinder with radius 25.4 cm in radius, 25.4 cm high, having 22 radial intervals and 22 axial intervals. The top two and bottom two axial intervals and the outermost two radial intervals used steel cross sections; the others were LiH. An asymmetric 100-angle quadrature set with 76 downward and 24 upward angles was selected in an attempt to prevent ray effects. The spacial mesh was nonuniform, but a rule was followed that no interval be more than twice as wide as its neighbor.

The source was represented by a top boundary source in the first six downward angles. The source varied with energy group according to the measured source spectrum and with radial interval according to the measured beam profile.

In the DUCT calculations, the duct was represented by a cylinder 2.54 cm in radius completly penetrating the shield with its axis coinciding with the axis-of-symmetry of the shield. The rest of the geometry of the shield was input to the GEOM package, with the requirement that the duct be re-input as the first quadratic surface for GEOM.

DUCT calculations were run for three detector positions with shield, sodium, or void in the duct. In each case the objective is to calculate the flux crossing the duct wall or colliding within the duct and reaching the detector.

To "know" the unperturbed flux at the detector location requires that it be available from the DOT calculation. For detectors at or in the shield, simple interpolation of the DOT fluxes will

suffice. For detectors near the shield it is therefore recommended that the DOT calculation contain void intervals which themselves contain the proposed detector sites. For detectors far from the shield, surface integration of the DOT fluxes and their projection to the detector, such as is done in DASH is required to determine the unperturbed flux.

3.1 COMPARISON WITH MONTE CARLO CALCULATION

A MORSE (ref. 4) Monte Carlo calculation was performed for the experimental configuration with sodium in the duct. Detector No. 1 was represented by a point one inch from the shield on the duct axis. The scattered flux was calculated by last-flight estimation from each collision site. The source was represented by a circular beam six inches in radius with its center on the duct axis. The general O5R geometry package (GEOM) was used.

The final calculation involved 84 batches of 100 neutrons each. Each neutron started from some point in the 6-in. radius circle on the top surface of the shield. Its distance from the center of the circle was selected uniformly from 0 in. to 6 in. and its weight adjusted by

$$\text{WATE} = 2*\text{WATE}*\text{RADIUS}/\text{BEAM},$$

where RADIUS is its distance and BEAM = 6 in., to account for the fact that the circular area was not sampled uniformly. Its direction from the center of the circle was selected randomly. Its starting direction cosines were (0, 0, 1), that is, normal incidence.

The initial energy group of the neutron was selected from the 15 groups not according to the natural source energy distribution but from a biased distribution which favored the higher energy groups; MORSE adjusted its weight to compensate for the source biasing.

The path length of each flight was selected not from the natural exponential distribution but from a transformed exponential distribution which encouraged longer paths near the the favored downward direction and shorter paths near the upward direction. The parameter PATH = 0.5 was used; MORSE adjusts the weight to account for the path length biasing.

At the end of each flight path is a collision site; since absorption is not allowed, the neutron's weight is suitably multiplied by a nonabsorption probability. A last-flight estimate is then made, contributing

$$P(\theta)*\text{WATE}*\text{EXP}(-\text{ARG})/R^2$$

to the scalar scattered flux at the detector for every energy group into which the neutron could possibly scatter from its present group. Then the neutron is allowed to launch its next flight in a newly determined direction with path length selected from the transformed exponential distribution.

At the end of the 84 batches, the scattered flux and its fractional standard deviation were calculated for each energy group, the scattered flux was added to the direct flux, and the results divided by the group width in MeV. The final units of the flux were (neutrons/cm^2-MeV)/(Incident neutron-cm^{-2}). Eighty thousand, four-hundred eighty-two scattering events contributed to the flux estimates. The fractional standard deviation of the scattered flux ranged from 5 to 20 percent.

A comparison with the DUCT calculation is shown in fig. 1. In general, the agreement varies between 10 to 20 percent, with the DUCT calculations consistently higher, except for the lowest two energy groups.

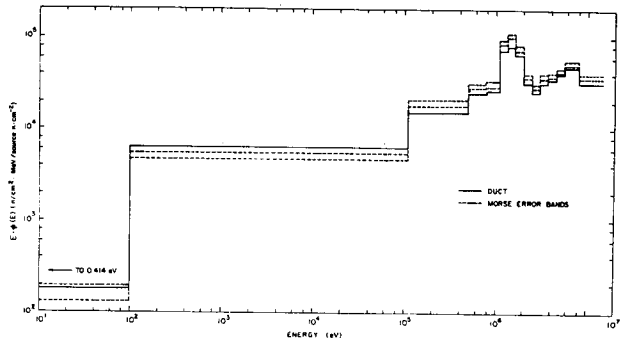

Fig. 1. Comparison between DUCT and MORSE calculated axial responses

4. EXPERIMENTAL PROGRAM

The experiments were designed to be as sensitive as possible to streaming but "clean" enough to provide a good check on the analysis.

4.1 NEUTRON SOURCE

The experimental layout for the experiments is shown in fig. 2. Photo-neutrons were produced in the tantalum-beryllium converter bombarded by 50-MeV electrons from the Gulf Radiation Technology linear accelerator. This converter has been used in several previous programs (ref. 5) at Rad Tech and provides the source spectrum shown in fig. 3. This is the spectrum measured by time of flight over 50 meters; 2.54 cm of lead and 3.144 cm of uranium were used as filters at the 16-meter station to reduce the gamma flash. This setup is for the lithium-hydride-sodium duct experiments. A similar setup was used for the BATH-NERVA shield streaming experiments with the exception that the measurements were made at 16.7 meters. Neutrons produced in the tantalum-beryllium target were then collimated to provide a circular plane beam for normal incidence on the shield assembly.

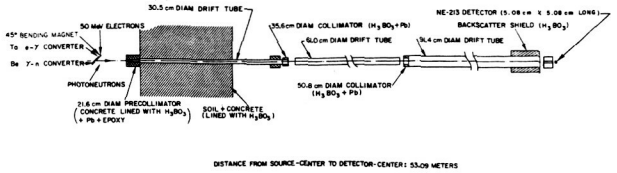

Fig. 2. Experimental layout for the lithium hydride duct *shield experiment*

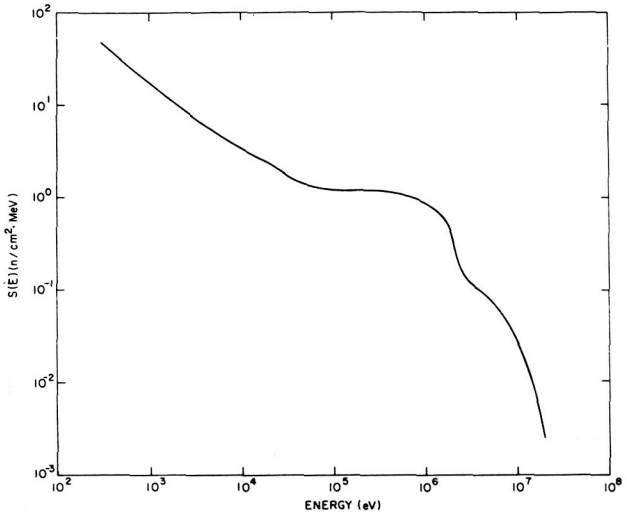

Fig. 3. Measured source spectrum for the lithium hydride duct shield experiment

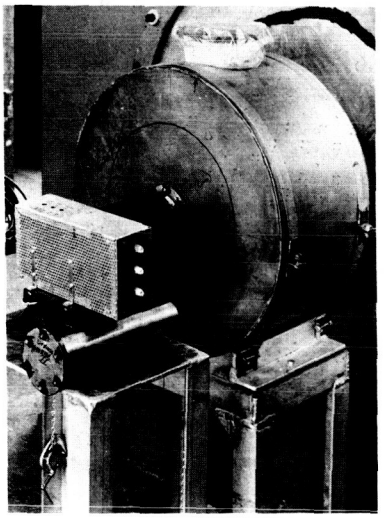

Fig. 4. Lithium Hydride Duct Shield Assembly.

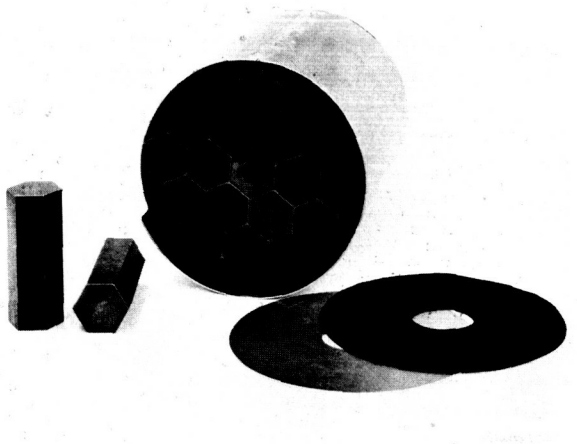

Fig. 5. Inner-BATH Shield Assembly.

4.2 SHIELD ASSEMBLIES

Two shield assemblies were studied. The first assembly was cylindrical lithium hydride assembly 50.8 cm in diameter by 25.4 cm thick with a 5.08 cm diameter axial duct. The assembly in situ at the end of the 50-meter flight path is shown in fig. 4. The duct was filled with either sodium or lithium hydride.

The BATH assembly consists of nineteen two-in. hexagonal by 11-in. long pieces, placed in an hexagonal matrix approximately 10 inches diameter by 11.1 inches long. To minimize the effect of room-return neutrons, the matrix was enclosed in a 10-in. diameter cylindrical container enclosed by a 5-in. thick shield. The shield consisted of a mixture of 50% by weight of lithium carbonate (Li_2CO_3) and polyethylene (CH_2). The inner BATH assembly is shown in fig. 5; the assembled BATH and side shield in situ at the end of the 16-meter flight path is shown in fig. 6.

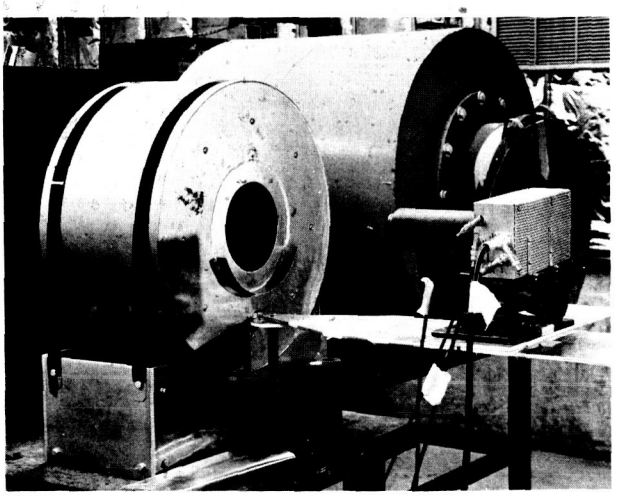

Figure 6. BATH Shield Assembly Enclosed in Outer Shield

4.3 DATA ACQUISITION

During a previous Rad Tech program (ref. 5), a new experimental method was developed for studying simultaneously fast-neutron transport and secondary gamma-ray production and transport in shields. With this method, an electron accelerator is used to produce intense 50-nsec pulses of photoneutrons. These neutrons stream down an evacuated 52-meter long drift tube to strike a shield assembly. An NE-213 detector is positioned immediately behind the shield assembly to detect both fast neutrons and secondary gamma rays produced in a shield assembly by $(n, x\gamma)$ and $(n, x\gamma)$ reactions.

A simplified block diagram of the three-parameter data acquisition system used with the NE-213 detector is shown in fig. 7. Three parameters, t, h, and x, are recorded for each detection event. The time parameter t is the time interval between the Linac pulse and the detection event; the pulse-height parameter h is proportional to the light produced in the NE-213 scintillator by neutron and gamma-ray interactions; and the pulse-shape discrimination parameter x identifies detection events as due to neutrons or gamma rays. The key features of each parameter are discussed next.

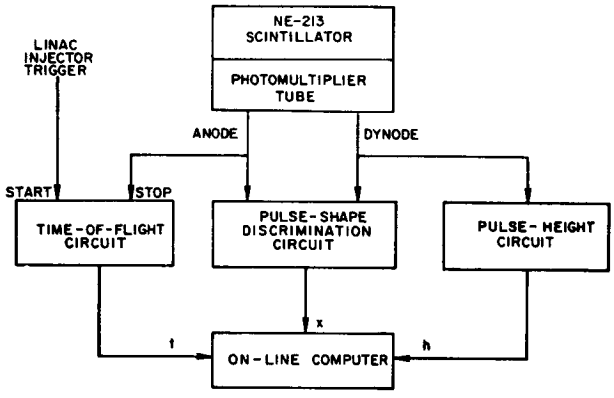

Fig. 7. Simplified diagram of the three-parameter data acquisition system

4.3.1 Time Parameter

The time parameter is related to the energies of neutrons incident on the shield assembly rather than the energies of neutrons leaking from the shield. This is true because the shield assembly is located at the end of the flight path near the detector rather than at the beginning near the pulsed neutron source as it would be for a conventional time-of-flight shielding experiment. The present geometry arrangement is also used for $(n, x\gamma)$ and (n, γ) reaction studies (ref. 6).

The time scale may be naturally divided into two regions. For short times ($t < 4$ μsec), detection events due to: (1) neutrons with energies above the detector threshold at 0.9 MeV ($t = 4.0$ μsec), and (2) gamma rays produced by $(n, x\gamma)$ reactions with threshold at 1.3 MeV ($t = 3.3$ μsec) are recorded. These events may be analyzed and interpreted in either the time domain or incident neutron energy domain. The results are completely equivalent within the abovementioned approximation.

However, for long times ($t > 4$ μsec), neutrons are not detected and only gamma rays produced by (n, γ) reactions are detected. Because these reactions may be due to uncollided neutrons, slowing-down neutrons, and/or thermalized neutrons, time and incident neutron energy cannot be uniquely related. Thus, these data are analyzed only in the long time domain. In summary, the data which are obtainable are categorized as due to:

1. Short time or fast neutrons ($E > 0.8$ MeV, $t < 4.0$ μsec)
2. Short time $(n, x\gamma)$ or inelastic gamma rays ($t < 3.3$ μsec)
3. Long time (n, γ) or capture gamma rays ($t > 3.3$ μsec).

4.4 UNFOLDING

The mathematical procedure for unfolding is carried out in the FERDOR code. The method is discussed in refs. 7 and 8. The results presented here are only the output from the FERDOR code. Each unfolded spectrum is not uniquely defined but instead gives a band of values within which the actual spectrum should lie.

The calculation of this band by FERDOR includes two contributions, one due to the statistical errors in the input pulse-height data, and the other to the suboptimal calculation of the "inverse" of the response matrix, because, in general, such errors are: (1) difficult to assess due to the indirect manner in which response matrices are produced by interpolation from calculation, and a measurement for example, and (2) difficult to propagate through the unfolding procedure. In our case, the response matrix was obtained entirely from a Monte Carlo O6R calculation performed at the Oak Ridge National Laboratory.

An excellent check on the methods described in the previous section is provided by the time-of-flight spectrum. Note that this spectrum is always measured simutlaneously by the three-parameter data acquisition system. The measured source spectrum (no shield assembly) obtained by time of flight should agree with that obtained by unfolding the proton pulse height spectra. A comparison is shown in fig. 8; the agreement is very good, which lends confidence to the unfolding procedure used here.

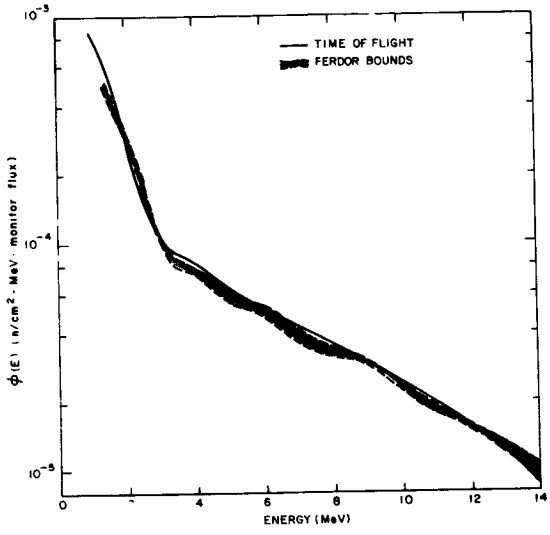

Fig. 8. Comparison between the FERDOR unfolded and time-of-flight measured source spectra

5. COMPARISON OF DUCT CALCULATION AND EXPERIMENT

Comparisons between the experimental data obtained with the lithium hydride assembly and calculations performed with the DUCT code are shown in figs. 9, 10, and 11. The calculations yielded neutron flux per MeV per source neutron; the measurements yielded neutron flux per MeV per source monitor. To compare the two on a source neutron basis, the measured results were multiplied by a source normalization factor. This factor was obtained by integrating the calculational source spectrum and the measured source spectrum over the same energy limits; namely, 2.0 MeV to 5.5 MeV, and then dividing the calculational source integral by the experimental source integral, that is

$$N_s = \frac{\left[\int_{2.0}^{5.5} \varphi(E)dE\right]_{DOT}}{\left[\int_{2.0}^{5.5} \varphi(E)dE\right]_{EXP}} = 0.674 .$$

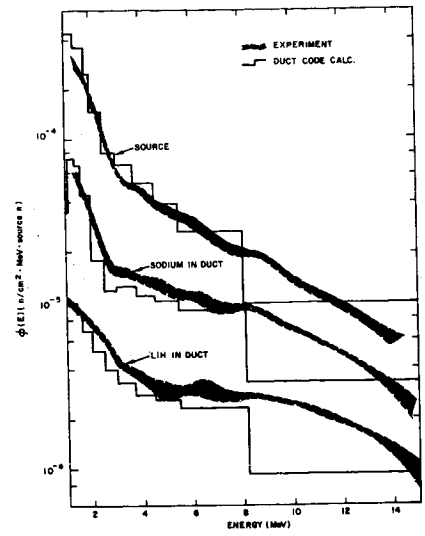

Fig. 9. Comparison between measured and DUCT calculated axial detector responses for a detector located at the duct exit

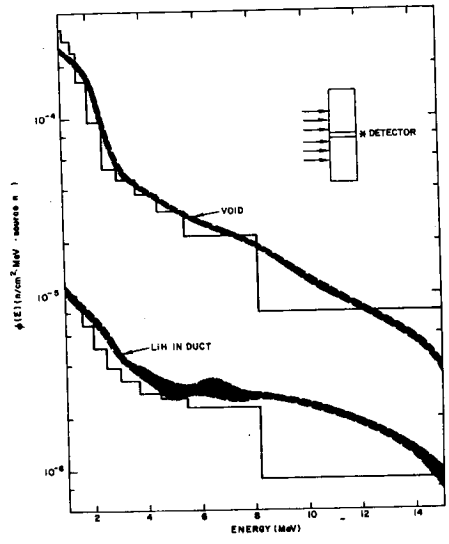

Fig. 10. Comparison between measured and DUCT calculated axial detector responses for a detector located at the duct exit

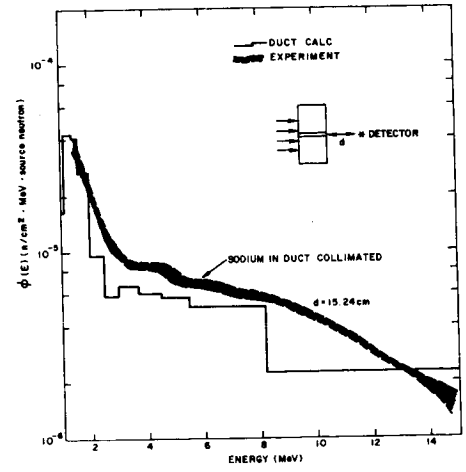

Fig. 11. Comparison between measured and DUCT calculated axial detector responses for a detector located 15.24 cm from the duct exit

This was done for the source spectrum only so that no further normalization is applied when comparing measurement with theory.

The comparison between the measured and axial detector responses is shown in fig. 9 for the sodium and lithium hydride filled ducts. Figure 10 compares the measured and calculated fluxes for void and lithium hydride filled ducts. Figure 11 compares the calculated and measured axial detector respones for a collimated detector located 12.7 cm from the duct exit. The final results for the BATH experiment-calculation comparisons are not complete at this writing.

6. CONCLUSIONS

In view of the overall agreement between measurement, DUCT and MORSE, we feel the DUCT code provides a good engineering code to claculate the effect of coolant type holes in shields. We have tested the method to its extreme limit for streaming.

The experiments were limited to neutron energies above 1 MeV; however, as noted earlier, the agreement with MORSE was very good at the low energies ($E < 10$ keV) where the fluxes tend to be isotropic lending confidence to the DUCT calculations at these energies. It is important to note that the MORSE calculation required approximately 30 to 45 minutes to achieve a 10 to 20% variance on the scattered flux estimates for a single detector position. The DUCT calculations require approximately four minutes per detector with an additional 40 to 60 minutes for the DOT calculation. However, if one were making an engineering type analysis of a shield where many duct-detector configurations are to be studied, the DOT-DUCT running time would be considerably shorter than the MORSE running time, as seen in the following table:

MORSE VS DOT/DUCT RUNNING TIMES PER DETECTOR (min)

Number of Ducts	1	2	4	6
MORSE	40	80	160	240
DOT/DUCT	64	68	72	80

We recommend that a void region be included in the DOT calculation for detectors near the shield/void region to minimize errors in extrapolating the DOT fluxes. For detectors quite distant from the shield, we recommend the use of DASH, which we plan to incorporate in the production version of DUCT.

ACKNOWLEDGEMENTS

The support of the U. S. Atomic Energy Commission under Contract AT(04-3)-167 is gratefully acknowledged.

REFERENCES

1. W. E. Selph, et al., Weapon Shielding Handbook, Chapter 5, Methods of Calculating Effects of Ducts, Access Ways, and Holes in Shields, DASA Report DASA-1891-1, January 1969.

2. K. D. Lathrop, "Theory and Use of the General-Geometry TWOTRAN Program," Los Alamos Scientific Laboratory Report LA-4432 (1968).

3. F. Mynatt, "DOT, A Two-Dimensional Discrete Ordinates Transport Code," CCC-89 K-1694, Oak Ridge National Laboratory - Radiation Shielding Information Center (1969).

4. E. A. Straker, et al., "The MORSE Code, A Multigroup Neutron and Gamma-Ray Monte Carlo Transport Code," Oak Ridge National Laboratory Report ORNL-485, September 1970.

5. L. Harris and H. Kendrick, "Time-Dependent Fast Neutron and Secondary Gamma-Ray Spectrum Measurements in Concrete," DASA Report 2401-1, Gulf General Atomic Incorporated (1969).

6. V. J. Orphan and C. G. Hoot, "Measurement of Gamma-Ray Production Cross Sections for Nitrogen and Oxygen," DASA Report DASA 2267, Gulf General Atomic Incorporated (1969).

7. W. R. Burrus and V. V. Verbinski, Nucl. Instr. Methods 67, 181 (1969).

8. V. V. Verbinski, et al., Nucl. Instr. Methods 65, 8 (1968).